31st Annual International Conference of the IEEE EMBS
Minneapolis, Minnesota, USA, September 2-6, 2009

Electrocardiographic Inverse Problem: Spatial Characterization of the Left Ventricle Potential

Matti Stenroos and Lauri Toivonen

Abstract— **In this work, we present a method for spatial characterization of the electrical activity of the left ventricle (LV). The presented method, electrocardiographic LV imaging, aims at characterization of main morphological features of the LV electrical activity via simple inverse reconstruction of the electrocardiogram on a standard LV segment model. The method is demonstrated with a case study dealing with the spatial characterization of an old myocardial infarction (MI). The results are encouraging: the centroid of the MI region is localized correctly, and the shape of the reconstructed infarcted region is similar to that in the golden standard solution, even though a patient-specific thorax model was not used.**

I. INTRODUCTION

In electrocardiographic imaging (ECGI), cardiac electrophysiology is assessed by solving the inverse problem of electrocardiography, applying body surface potential mapping (BSPM) and volume-conductor modeling. The two main approaches to ECGI are source modeling and epicardial potential imaging. In source modeling, the aim is to reconstruct the primary source (transmembrane potential) distribution or an equivalent source that is assumed to reflect the behavior of the sources. In epicardial potential imaging, the electric potential outside but near the source region is reconstructed without any reference to the sources, aiming at simulation of epicardial electrograms or at indirect localization of cardiac sources.

Although the logic and principles of these two approaches to the cardiac inverse problem are different, both approaches are typically used in connection with boundary-element (BEM) modeling of the thorax. The essential computational difference in the BEM forward modeling between these approaches is that in source-modeling, the forward transfer function is constructed with double-layer integral operators and a source model, while in epicardial potential imaging, both double- and single-layer integrals operators are needed, but no source model is used [1]. The presence of single-layer integrals makes the epicardial potential problem computationally more challenging than the source-modeling problem. But, with epicardial potential imaging, one is reconstructing a physical potential distribution instead of an equivalent model, enabling a more general solution that is less dependent on a priori assumptions than solutions obtained with the source-modeling approach.

M. Stenroos is with Department of Biomedical Engineering and Computational Science, Helsinki University of Tehchnology, P.O. Box 2200, FI-02015 TKK, Finland. matti.stenroos@tkk.fi

L. Toivonen is with Division of Cardiology, Helsinki University Central Hospital, P.O. Box 340, FI-00029 HUCH, Finland. lauri.toivonen@hus.fi

In studies carried out, e.g., by the Tilg [2, 3] and Rudy [4, 5] research groups, the performance of these approaches has been comparable. In both approaches, patient-specific modeling of the thoracic volume conductor is essential, requiring accurate imaging information obtained with magnetic resonance imaging (MRI) or X-ray computed tomography (CT). In most studies of epicardial potential imaging, the lungs have been omitted from the model. Including the lungs will improve the results further [1, 6, 7]. While our recent results show that the Galerkin BEM is more accurate and stable in the epicardial potential problem than the conventionally used collocation BEM, the bottlenecks in the inverse problem of electrocardiography are in volume conductor modeling and especially in regularization of the inverse problem [1], not in the methodology of numerical field calculation.

In this paper, we study a simplified approach to the electrocardiographic inverse problem that yields clinically usable information also without accurate volume conductor models. We call such simplifying approaches "spatial characterization of the electrocardiogram", pinpointing that the aim is, instead of reproducing accurate source or potential distributions, to characterize the main morphological features of the electrocardiogram with respect to cardiac anatomy.

II. ECG IMAGING OF LEFT VENTRICLE

Anatomical and functional information on the left ventricle (LV) is typically assessed with help of an LV segmentation, such as the one proposed by the American Heart Association (AHA) [8]. In the AHA segmentation, the left ventricle is divided into 17 segments (basal anterior, mid inferior, apical septal, etc.). The AHA segments can be visualized on a semi-ellipsoid, with long axis pointing in the direction of the anatomical LV axis. As clinicians are familiar with interpreting the LV function in terms of the AHA segments, we believe that it would be worthwhile to present electrocardiographic variables in connection with the AHA segmentation. Such a presentation would especially facilitate the understanding and interpretation of body surface potential mapping data.

The inverse reconstruction of ECG data from body surface to the LV ellipsoid can be carried out with either source-modeling or potential-imaging approaches. The LV segments can be used either as template regions of predefined source/potential or as anatomical guidelines in the visualization of reconstructed source or potential distributions. When the segments are used as templates, a source or a potential model is spanned according to the segments, leading to the degree-of-freedom of 17 for the LV electrical

978-1-4244-3296-7/09/$25.00 ©2009 IEEE

activity. In segment-based source-modeling, a unit-strength source (double-layer, single-layer, dipole, monopole, etc.) is assigned to each segment. A lead vector representing the relationship between the source amplitude and the generated ECG is constructed for each segment, and the ECG is modeled as a linear combination of these lead vectors,

$$\mathbf{\Phi} = \mathbf{L}\mathbf{s},$$

where $\mathbf{\Phi}$ is the body surface potential at electrode locations, $\mathbf{s}$ is the 17×1 vector of source amplitudes, and columns of the lead field matrix $\mathbf{L}$ contain the lead vectors for all source components. The same lead-vector approach (with different kernel $\mathbf{L}$, of course) applies to the segment-based potential templates as well, although the concept of lead-field is more commonly used in connection with source-modeling.

The inverse reconstruction can be carried out either via regularized inversion of the matrix $\mathbf{L}$ (see, e.g., [9]) or with help of iterated forward solutions. Prior knowledge on source or potential distribution can be brought in statistically [6] or with the simple template approach [10].

The most simple way to utilize the LV segmentation in spatial characterization of the ECG is to search for the single segment that best correlates with the measured ECG. Overall, a single-segment source or potential model is physiologically of limited value, and the corresponding surface potential does typically not reproduce the measured ECG well. With some a priori information and a proper clinical question, such a simple model can, however, provide clinically useful information. For example, focal LV ectopic activity could be coarsely localized by iteratively searching, which segment produces the double-layer potential that best correlates with the beginning of the QRS complex in the measured ECG. This localization result can be used in guiding of the ablation catheter towards the arrhythmogenic tissue. Or, the centroid of a compact transmural ischemic lesion can be localized with help of a segment of positive potential that has a region of negative potential around its boundaries (see [10]).

A. Methods and Results

We have implemented both source-modeling and potential-imaging approaches of the electrocardiographic LV-imaging. In both approaches, we used the Dalhousie thorax model [11] with lungs and right-ventricular blood as conductivity inhomogeneities. A semi-ellipsoidal mesh was fitted manually to the model according to anatomical directions presented in [8]. The resulting model is visualized in Fig. 1. The forward model for the source-modeling problem was constructed with the Helsinki BEM library [12], and for the LV potential as described in [7].

In the first tests, different single-segment approaches produced logical and similar results. Of reconstructions over all segments (Tikhonov 0-regularized inversion of the lead field matrix $\mathbf{L}$), those obtained with source-model kernels were more scattered and difficult to interpret than the corresponding ones obtained with the potential-imaging kernel. When the LV potential was reconstructed with help of the Tikhonov 2 regularization on the (closed) semi-ellipsoidal

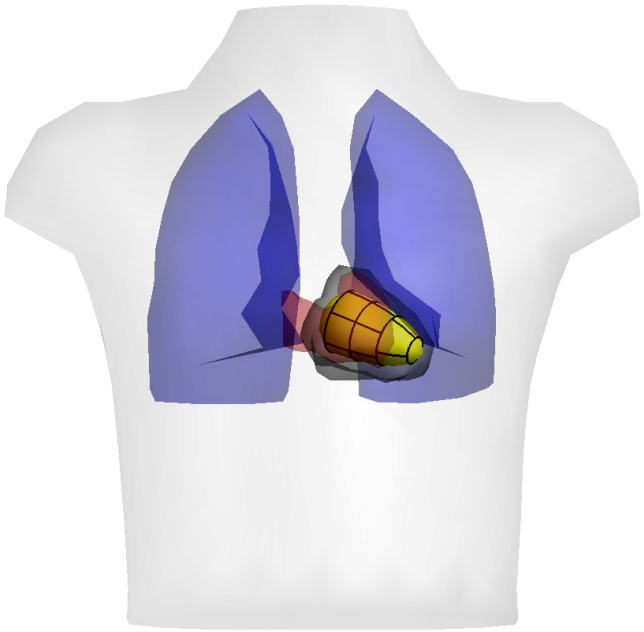

Fig. 1. The thorax model used in the inverse reconstruction of LV electrical activity.

mesh comprising 206 nodes and 408 elements and visualized on the mesh together with the AHA segment boundaries, the results were morphologically much smoother than those computed with the segment-based approach (see the right column of Fig. 2). This was not only an issue of better visualization and interpolation; the spatial behavior (potential gradients, sign changes) was overall smoother in the mesh-based reconstruction than in the segment-based one. Because of the most convincing first results, the mesh-based reconstruction of LV potential was studied further.

We demonstrate the LV potential imaging with case 1 of the Computers in Cardiology Challenge 2007 dataset [13, 14]. The set comprises BSPM recordings and contrast-enhanced cardiac magnetic resonance images obtained from patients with an old, relatively compact myocardial infarction (MI), and the aim of the challenge was to characterize the extent and location of the MI in terms of the AHA segmentation. The reference results, interpreted from the MRI data, were given as a list of infarcted segments. The case was studied as an independent test case; reference results were not consulted before analysis, and methods and algorithms were not tailored in order to better match the reference. The positions of the 123 BSPM electrodes were given in terms of the Dalhousie thorax model, making the analysis of the BSPM data with our model straightforward.

The BSPM raw data were first visually inspected, spotting a Q wave in many frontal leads and an overall fragmented beginning of the QRS complex. The baseline was set to PQ segment and the beginning and end of the QRS were set manually. Based on the presence of the Q wave, the time-integral of the first quarter of the QRS was chosen as the feature used for reconstruction of the LV potential. The QRS

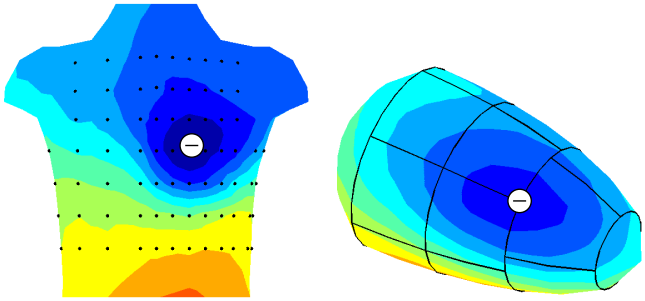

Fig. 2. The QRS first-quarter-integral map from a MI patient (on left) and the corresponding inverse reconstruction of the LV potential (on right). The minimum of each map is marked with a "-"-sign. The dots on the thorax surface illustrate the locations of the ECG electrodes, and the AHA segmentation is displayed with the grid on the LV model.

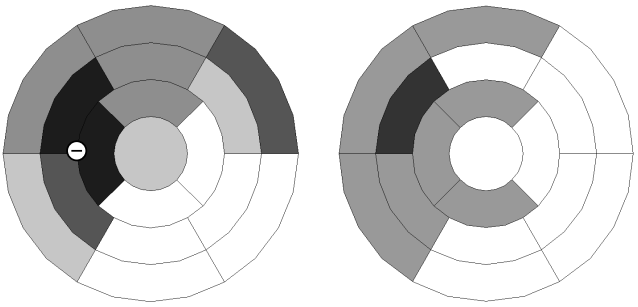

Fig. 3. The LV potential reconstruction of a MI patient and the reference result, visualized in bullseye layout. Left: the region of negative potential in the inverse reconstruction, in which darker colors indicate more negative potentials. Right: the golden standard MRI result, in which the gray and black segments mark the infarction area, the black segment containing the maximal damage.

quarter-integral map is visualized in the left column of Fig. 2. The map shows strong negative amplitudes on the anterior thorax, corresponding to the negative Q integral in the anterior leads. The inverse reconstruction was done with help of the Tikhonov 2 regularization, setting the regularization parameter so that the goodness-of-fit of the body surface data was close to 0.95, as was done also in [10]. The resulting LV potential distribution is visualized in the right column of Fig. 2. The strongest negative potentials, reflecting the location of the tissue contributing most to the Q wave, were obtained in the mid- and apical anterolateral segments and in the basal lateral region.

In the left column of Fig. 3, the negative part of the segment-average of the reconstructed potential is visualized on a circumferential polar (a bullseye) plot oriented as in Fig. 4 of [8]. This simple visualization method allows a quick interpretation of the result in terms of the AHA segments. In the right column, the reference result is illustrated. The morphology of our reconstruction is similar to the reference: the region of the strongest negative potential matches the given centroid of the MI region, and the shape of the reconstruction is in good morphological correlation with the reference, although the reconstruction extends too far to the basal lateral part, and in the apical region, the reconstruction should extend further to the inferior wall. A slight re-orientation of the LV mesh would improve the estimation of the edges of the infarcted region in this example case, but at the same time it could weaken the accuracy of localizing the center of the infarction.

III. DISCUSSION

In LV potential imaging of the MI patient case, the centroid and shape of the MI region were characterized correctly, while the extent of the infarcted region was estimated too large in the basal region. Taking into account that the case was done in a blind-test manner—no patient-specific anatomy was used and no parameters were tailored in order to better match the reference—the result is very satisfactory. In the example case, the results could be improved by optimizing the ECG feature extraction and post-processing of the reconstruction. Overall, to specify the optimal ECG feature and analysis technique and to assess the diagnostic performance of estimating the MI size (or of some other specific task) would demand further studies with a large dataset. We, however, believe that LV potential imaging can help in interpretation of the spatial features of the electrocardiogram also without optimized criteria and dedicated analysis methods. Being able to show the relationship between the potential in a well-specified cardiac region and the corresponding body surface potential distribution, it can be a helpful tool in ECG education, too.

The use of the LV ellipsoid as the surface of reconstructed potential or source omits the sources in the right ventricle. In the source-free potential problem it is assumed that all sources are inside the reconstruction surface [1]mathematically speaking, the LV potential reconstruction is thus not valid. In practice, the RV activity corrupts the LV potentials at least on the septal wall; with data containing significant RV contribution, the overall morphology of the Tikhonov-regularized LV potential reconstruction will be similar to the corresponding epicardial potential, increasing the risk of misinterpretation. The LV potential imaging is hence suited only to applications, in which the role of the right ventricle can be assumed negligible.

Although our original idea of the electrocardiographic LV imaging was to characterize the LV electrical activity without any patient-specific model information, the presented method would benefit from a tailored volume conductor model; patient-specific positioning and especially orientation of the heart and ellipsoid relative to the electrodes would improve the results. In addition to MRI or CT scans, such information could be extracted with help of statistical image processing from biplanar thoracic X-ray pictures—anatomical data that are often available also in situations, in which the tomograhic imaging data or facilies aren't.

If thoracic MRI needs to be performed in order to construct a proper volume conductor model, the need of making a BSPM measurement and solving the inverse problem in order to characterize, e.g., an acute myocardial infarction may be questioned: the anatomical MRI scan can be accompanied

with cardiac MR sequences, allowing the characterization of ischemic lesions or MI scars. It is hence easy to understand that in inverse ECG studies, the weight has been on tasks that can't be carried out with cardiac MRI, such as localization of the earliest ventricular activation. Solving the ECG inverse problem can, however, be motivated, even if standard diagnostic information is already available— additional information can be used for confirming or questioning the diagnosis or for planning the treatment. When the standard diagnostic information is obtained with MRI or some other tomographic method, the LV potential imaging, compared to the other approaches to ECG inverse problem, has the benefit of displaying the electrophysiologic data in the same frame of reference with the tomographic information, allowing also quantitative analysis.

In our future work, we aim to analyze the full dataset [14] and experiment with tailored heart positioning. The LV potential imaging will also be further developed and applied with our existing datasets such as the one used in [10].

IV. ACKNOWLEDGMENTS

The authors thank Milan Horáček from the Dalhousie University for the thorax model.

REFERENCES

[1] M. Stenroos and J. Haueisen, "Boundary element computations in the forward and inverse problem of electrocardiography: Comparison of collocation and Galerkin weightings," *IEEE Trans. Biomed. Eng.*, vol. 55, pp. 2124–2133, Sep. 2008.

[2] R. Modre, B. Tilg, G. Fischer, F. Hanser, B. Messnarz, M. Seger, M. Schocke, T. Berger, F. Hintringer, and F. Roithinger, "Atrial noninvasive activation mapping of paced rhythm data," *J. Cardiovasc. Electrophysiol.*, vol. 14, pp. 1–8, 2003.

[3] R. Modre, B. Tilg, G. Fischer, F. Hanser, B. Messnarz, M. Seger, F. Hintringer, and F. Roithinger, "Ventricular surface activation time imaging from electrocardiogram mapping data," *Med. Biol. Eng. Comput.*, vol. 42, pp. 146–150, 2004.

[4] R. Ghanem, P. Jia, C. Ramanathan, K. Ruy, A. Markowitz, and Y. Rudy, "Noninvasive electrocardiographic imaging (ECGI): Comparison to intraoperative mapping in patients," *Heart Rhythm*, vol. 2, pp. 339–354, 2005.

[5] S. Ghosh and Y. Rudy, "Accuracy of quadratic versus linear interpolation in noninvasive electrocardiographic imaging (ECGI)," *Ann. Biomed. Eng*, vol. 33, pp. 1187–1201, 2005.

[6] A. van Oosterom, "The use of the spatial covariance in computing pericardial potentials," *IEEE Trans. Biomed. Eng.*, vol. 46, pp. 778–787, 1999.

[7] M. Stenroos, "Transfer matrix for epicardial potential in a piecewise homogeneous thorax model: the boundary element formulation," *Submitted*, 2009.

[8] M. Cerqueira, N. Weissman, V. Dilsizian, A. Jacobs, S. Kaul, W. Laskey, D. Pennell, J. Rumberger, T. Ryan, and M. Verani, "Standardized myocardial segmentation and nomenclature for tomographic imaging of the heart: A statement for healthcare professionals from the cardiac imaging committee of the council on clinical cardiology of the American Heart Association," *Circ.*, vol. 105, pp. 539–542, 2002.

[9] F. Greensite, "Heart surface electrocardiographic inverse solutions," in *Modeling and Imaging of Bioelectrical Activity: Principles and Applications*, B. He, Ed. Kluwer Academic, 2004, pp. 119–160.

[10] M. Stenroos, H. Hänninen, M. Lindholm, I. Tierala, and T. Katila, "Lead field formulation for epicardial potential in electrocardiographic localization of acute myocardial ischemia," in *Proc. IFMBE, 3rd European Medical & Biological Engineering Conference, Prague*, vol. 11, 2005, pp. 2265–1 – 2265–5.

[11] B. Horáček and J. Clements, "The inverse problem of electrocardiography: A solution in terms of single- and double-layer sources on the epicardial surface," *Math. Biosci.*, vol. 144, pp. 119–154, 1997.

[12] M. Stenroos, V. Mäntynen, and J. Nenonen, "A Matlab library for solving quasi-static volume conduction problems using the boundary element method," *Comput. Methods Programs Biomed.*, vol. 88, pp. 256–263, 2007.

[13] A. L. Goldberger, L. A. N. Amaral, L. Glass, J. M. Hausdorff, P. C. Ivanov, R. G. Mark, J. E. Mietus, G. B. Moody, C.-K. Peng, and H. E. Stanley, "PhysioBank, PhysioToolkit, and PhysioNet: Components of a new research resource for complex physiologic signals," *Circ.*, vol. 101, no. 23, pp. e215–e220, 2000 (June 13), `http://circ.ahajournals.org/cgi/content/full/101/23/e215`.

[14] PhysioNet, "PhysioNet/Computers in Cardiology Challenge 2007: Electrocardiographic imaging of myocardial infarction," 2007, `http://www.physionet.org/challenge/2007/`.